Influence of CO_2 Purity on the Corrosion of Structural Alloys for Supercritical CO_2 Power Cycles

M.S. Walker and E.A. Withey
Sandia National Laboratories
Livermore, CA USA

Dr. Matthew Walker (mswalke@sandia.gov) is a Senior Member of the Technical Staff at Sandia National Laboratories California. He specializes in the interaction of materials with their environment and with other materials at high temperature. His current research interest is focused on the evaluation of structural alloys for use in advanced energy systems. Most prominent among these are evaluating alloy performance in supercritical CO_2, which cuts across a range of energy technologies including nuclear, fossil, as well as renewable. Prior to joining Sandia, he worked for 5 years as a Materials Scientist at the Alcoa research center in Pittsburgh, PA. While at Alcoa, he developed ceramic and metallic materials for operation within the aggressive environments of molten fluoride salt as well as in molten aluminum. Before joining Alcoa, he received a MS and PhD in Materials Science and Engineering at Carnegie Mellon University.

Dr. Elizabeth Withey (MS and PhD Materials Science and Engineering 2007 and 2009) is a staff member at Sandia National Laboratories, California working to qualify next generation materials. Dr. Withey avidly applies her materials science knowledge and practical characterization skills to help solve real-world materials problems. Previously she investigated and characterized interfaces in materials for energy production and the use of metallic thin films in diffusion welding of dissimilar metals. During graduate school at the University of California, Berkeley, Dr. Withey probed the limits of strength and mechanisms for deformation in compression of nanopillars in a transmission electron microscope.

ABSTRACT

Structural alloy corrosion is a major concern for the design and operation of Supercritical CO_2 power cycles. A critical shortcoming is that nearly all of the available alloy corrosion data was performed using high purity CO_2 (research grade - 99.999% purity), while a commercial scale system is likely to use industrial grade CO_2 with higher impurity concentrations (< 99.98% purity). Furthermore, experimental investigations have been predominantly focused on higher temperatures (> 600°C), and have often neglected to examine corrosion rates for alloys at lower temperatures relevant for sodium fast reactor energy conversion system applications. An experimental program was recently established to address these shortcomings. Results are presented from a series of 1000 hour CO_2 exposure experiments using both research purity and industrial purity CO_2 at two temperatures relevant to sodium fast reactor energy conversion systems (350°C and 600°C). The set of eight different structural alloys included in these experiments (F22, F91, 304H, 316H, 347H, 800H, HR120, and 617) were characterized for weight gain and surface oxide microstructure. Ongoing work will be described where corrosion rate / lifetime predictions and internal carburization are being evaluated using samples from these experiments as well as those from recently completed experiments at the same two temperatures in air.

1. INTRODUCTION

The supercritical carbon dioxide (sCO_2) Brayton Cycle has gained significant attention in the last decade as an advanced power cycle capable of achieving high efficiency power conversion; it represents a thermal to electric energy conversion system with an efficiency approaching 50% under the operating conditions required for advanced energy systems. Sandia National Laboratories, with support from the U.S. Department of Energy Office of Nuclear Energy (US DOE-NE), has been conducting research and development in order to deliver a Recompression Closed Brayton Cycle (RCBC) that is ready for commercialization. There are a wide range of materials related challenges that must be overcome for the success of this technology. Structural alloy corrosion is a major concern for the design and operation of Supercritical CO_2 power cycles.

Four critical shortcomings were identified with the available alloy corrosion data. The first is that nearly all of the available alloy corrosion data was performed using high purity CO_2 (research grade - 99.999% purity), while a commercial scale system is likely to use industrial grade CO_2 with higher impurity concentrations (< 99.98% purity). The second is that experimental investigations have been predominantly focused on higher temperatures (> 600°C), and have often neglected to examine corrosion rates for alloys at lower temperatures relevant for sodium fast reactor (SFR) energy conversion (EC) system applications. Third is that experimental investigations have been predominantly focused on characterizing surface oxidation, and have often neglected to examine samples for internal carburization. Finally, structural alloy corrosion has only been evaluated in terms of sample weight gain, rather than by the more useful metric of metal loss.

An experimental program was recently established to address these shortcomings. A test configuration was developed enabling long duration CO_2 exposure tests (1000 hours) in a range of gases (research grade CO_2, industrial grade CO_2, Air) at temperatures relevant to sodium fast reactor energy conversion systems (350°C and 600°C). The set of eight different structural alloys included in these experiments (F22, F91, 304H, 316H, 347H, 800H, HR120, and 617) are being characterized for weight gain, corrosion rate / lifetime predictions, internal carburization, and surface oxide microstructure. This paper provides a detailed overview for experiments completed in both grades of CO_2 at the two temperatures, where samples have been characterized for weight gain and surface oxide microstructure. Ongoing work will also be described where corrosion rate / lifetime predictions and internal carburization are being evaluated for samples from these same experiments as well as those from recently completed experiments at the same two temperatures in air. In addressing the identified shortcomings, information is being provided to design engineers that enable appropriate alloy selections for system components.

2. BACKGROUND

Analysis was completed in 2016 in making component alloy recommendations for an SFR 10MW energy conversion (EC) system design with a 550°C turbine inlet temperature (TIT) [1]. The process used for doing this analysis is shown in Figure 1. The exposure conditions in terms of temperature and pressure were established for all system components. Candidate alloys were identified which satisfy the mechanical strength requirements for each exposure condition. These candidate alloys were then evaluated based on their cost and corrosion performance, using the chart in Figure 2, in determining the best options for each exposure conditions. Based on this analysis, ferritic alloys G22 and G91 were recommended for all components at less than 400°C, while austenitic alloys 316H and 347H were recommended for all components above this temperature.

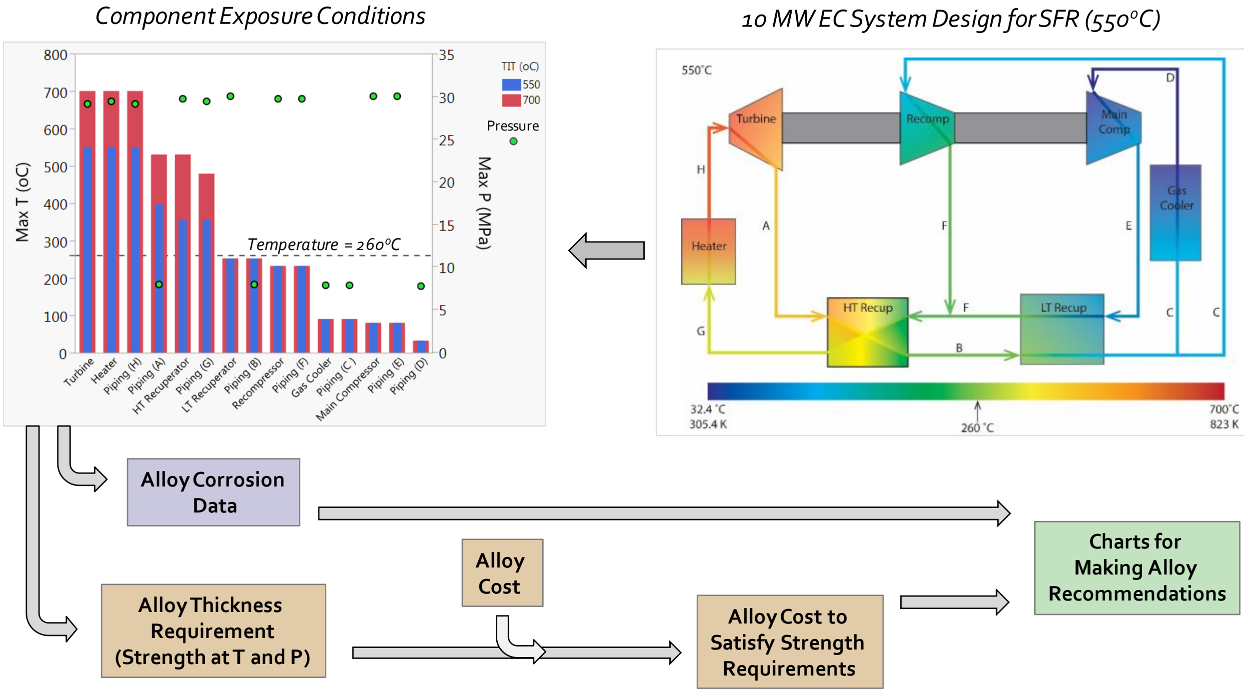

Figure 1. Process used in making alloy recommendations for a 10MW EC system design for SFR [1]

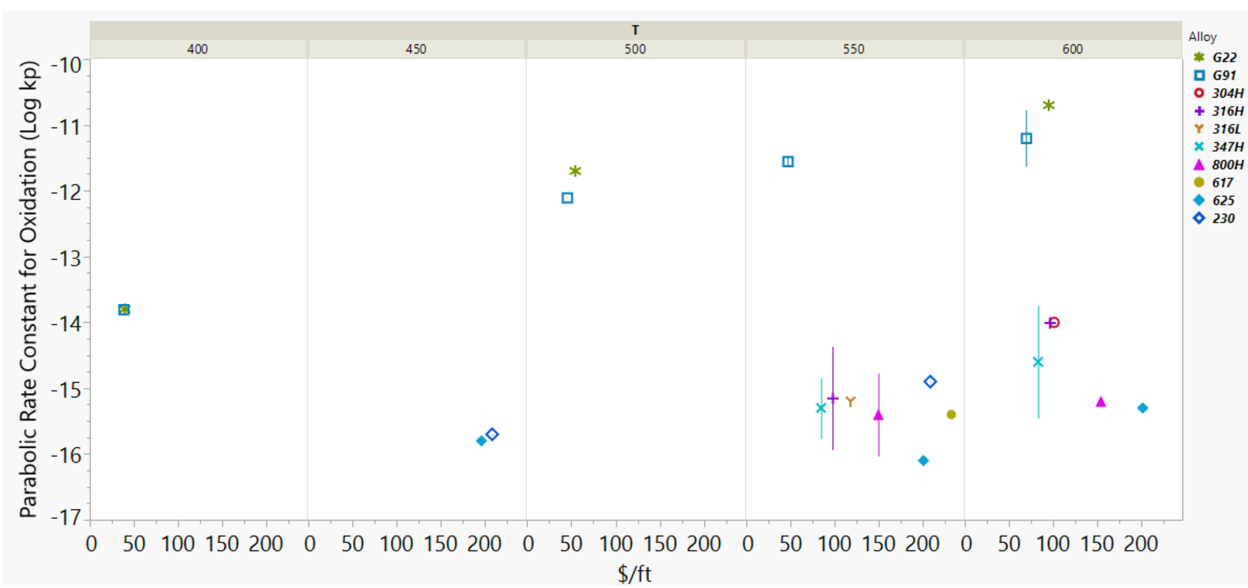

Figure 2. Candidate alloys compared by corrosion rate and cost for a range of temperatures [1]

There are several caveats in making these alloy recommendations. In order to validate alloy recommendations made previously, an experimental program was established that specifically addresses each of these caveats. There is very limited alloy corrosion data available at lower temperatures relevant for sodium fast reactor (SFR) energy conversion system applications. Also, this analysis only considered surface oxidation and not internal carburization, which appears to have been overlooked in the past as part of corrosion studies in CO_2. Furthermore, structural alloy corrosion has only been evaluated in terms of sample weight gain, rather than by the more useful metric of metal loss. Finally, all of the alloy corrosion data was obtained using research grade CO_2, while the lower purity industrial grade CO_2 will be used in a real system.

Considerable work was done in Japan (JAEA) to study the sCO_2 compatibility of 9Cr and conventional austenitic stainless steels (i.e. 316FR) for fuel claddings at 400°-600°C and 10-20 MPa. Unfortunately, they did not characterize carbon ingress[2]. More recently, others have begun to include this in their investigations. KAIST [3] found carbon ingress to be much higher on Fe-base alloy 800H compared to Ni-base alloys 600 and 690. Secondary ion mass spectroscopy data of alloys exposed for 1000 h at 600°C in 20 MPa sCO2 is shown in Figure 3. CSIRO [4] found the presence of internal carburization for 316, but not for the Nickel base alloy Hastelloy C276; they tested over the temperature range of 650-750°C, and so was done at higher temperatures than are relevant for an SFR EC system.

Some recent experimental work (ORNL [5], NETL [6], and Wisconsin [7]) has been initiated to understand the impact of gas chemistry on alloy corrosion. This work is focused on the higher temperatures (>650°C) used in fossil and solar heated sCO_2 systems, and it looks exclusively at a very limited set of gas impurity concentrations. Alloy corrosion behavior in these gas chemistries may change in moving to the lower temperatures used in a nuclear energy heated system.

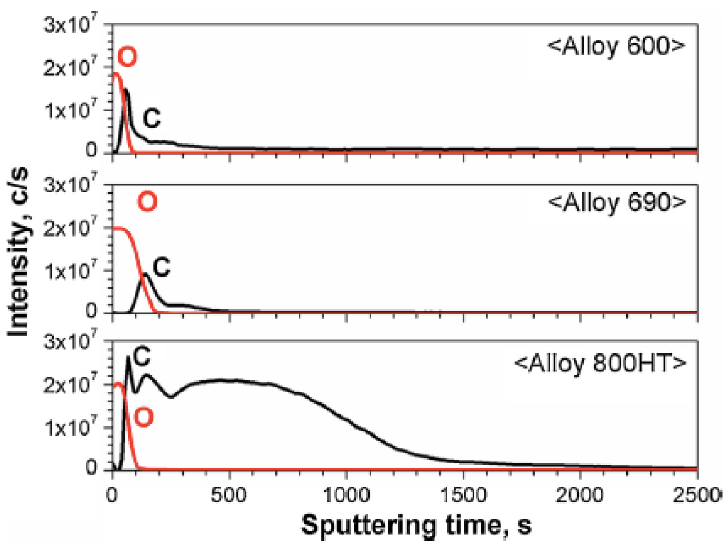

Figure 3. Carbon ingress for alloys exposed at 600°C in 20 MPa sCO_2 for 1000hrs [3]

3. EXPERIMENTAL APPROACH

Two large three-zone tube furnaces (3 feet length) have been set up to complete the alloy corrosion experiments at Sandia's laboratory in Livermore, CA. These experiments have been conducted at atmospheric CO_2 pressure, as recent results from others [6, 8] indicates that CO_2 gas pressure does not appear to influence alloy corrosion. All experiments are completed over 1000 hours' duration at both 350°C and 600°C, using eight different alloys from across the corrosion performance/cost spectrum (Grade 22, Grade 91, 304H, 316H, 347H, 800H, HR120 and 617). Similarly, to other experiments, samples of each alloy are pulled and analyzed for corrosion at 500 hour intervals. Experiments involved the use of two gas chemistries, covering the full range of expected gas impurities from the highest purity (research grade, >99.999%) to the lowest purity (industrial grade, < 99.98%). Additional experiments were completed in air in order to provide comparison for alloy behavior in terms of oxidation and carburization in an environment devoid of a carbon containing gas. Following completion of each experiment, a program has been established for analyzing samples for corrosion (weight gain as well as metal loss) and carbon ingress.

3.1. Materials

A group of eight different alloys were included in this investigation. Selection of these alloys was made based on covering the range of alloy categories / chemistries (ferritic Fe-base, austenitic Fe-base, and Ni-base), and consideration for alloys which are ASME Section III Division 5 approved. The alloys included in these experiments along with their measured chemistries are provided in Table 1. The ASME Sec III Div 5 alloys include F22, F91, 304H, 316H, 800H, and 617. Alloy 347H was included based on the merits of its corrosion/cost performance from the 2016 analysis[1]. Alloy HR120 was included based on it filling a unique chemistry space not occupied by any of the other alloys.

All alloy samples were provided by Metal Samples, Inc. (Munford, AL) with a 600 grit surface finish. Sample dimensions varied by alloy, based on what was most easily available by the vendor in preparing these samples. Sample dimensions for each of the alloys are shown in Table 2. Each sample was provided with a 1/6th inch hole for holding the samples within the furnace sample holder.

The two grades of CO_2 gas that have been used in these experiments are the higher purity research grade (RG) along with the lower purity industrial grade (IG). The use of both gases in these experiments provide the means for evaluating alloy corrosion across the full spectrum of gas chemistry that will be possible for an SFR EC system. Both gases were provided by Matheson Tri-Gas Inc. (Newark, CA). Chemical analysis for each of the gas cylinders used in these experiments are provided in Table 3. Experiments were designed such that one gas cylinder was used to complete each of the four 1000 hour experiments listed in this table. In this way, the complete gas chemistry for each experiment was known and remained consistent throughout the entire experiment. In the case of the 350°C – IG experiment, precise concentrations of N_2 and O_2 are not known as these exceeded the detection limits for these gases (indicated in the table). For experiments completed in air, cylinders of air were used with very low impurity concentrations (Ultra Zero Air).

Table 1. Chemical Analysis for Alloys

Alloy	Chemical Analysis (Wt %)																			
	Fe	Cr	Ni	Mn	Co	Mo	Si	Al	B	C	Cu	P	S	Ti	W	Nb	N	V	Zr	Ta
F22	98.13	2..19	0.07	0.4	-	0.95	0.2	0.021	0.0001	0.1	0.1	0.008	0.011	0.002	-	0.001	-	0.004	-	-
F91	89.25	8.38	0.18	0.43	-	0.94	0.32	0.011	-	0.1	-	0.02	0.01	0.007	-	0.067	0.063	0.22	0.001	-
304H	70.54	18.16	8.08	1.39	0.32	0.4	0.44	-	-	0.049	0.51	0.032	0.0004	-	-	-	0.081	-	-	-
316H	68.60	16.61	10.26	1.536	0.152	2.006	0.329	-	-	0.041	0.392	0.036	0.001	-	-	0.005	0.0315	-	-	-
347H	68.73	17.24	9.32	1.83	0.45	0.38	0.66	-	-	0.06	0.51	0.028	0.019	-	-	0.74	0.017	-	-	0.02
800H	46.70	20.56	30.6	0.54	0.03	-	0.32	0.52	-	0.07	0.03	0.12	0.0001	0.57	-	-	0.01	-	-	-
HR120	35.48	24.91	37	0.68	0.15	0.27	0.5	0.08	0.002	0.062	0.09	0.012	<0.002	<0.01	<0.1	0.6	0.163	-	-	-
617	0.76	22.63	53.2	0.02	12.33	9.38	0.15	1.15	0.002	0.06	0.05	-	0.001	0.27	-	-	-	-	-	-

Table 2. Corrosion Sample Dimensions

Alloy	Diameter (in)	Thickness (in)
F22	0.47	0.063
F91	1.25	0.063
304H	0.47	0.188
316H	0.47	0.125
347H	0.47	0.040
800H	0.50	0.063
HR120	0.47	0.063
617	0.61	0.063

Table 3. Chemical Analysis for CO_2 Gases

T, °C	CO_2 Grade	Gas Chemical Analysis						
		CO_2 (%)	CO (ppm)	H_2 (ppm)	N_2 (ppm)	O_2 (ppm)	CH_4 (ppm)	H_2O (ppm)
600	RG	> 99.999	0.054	0.021	3.097	0.110	0.355	< 0.02
350	RG	> 99.999	0.012	0.005	1.070	0.040	0.153	< 0.02
600	IG	> 99.98	< 0.010	0.040	35.370	11.110	0.430	0.53
350	IG	</= 99.98	< 0.010	0.040	> 80	> 60	0.420	0.81

3.2. Experimental Setup

In order to complete these experiments, two large tube furnaces were setup. Both furnaces have 3 heating zones and total length of 3 feet, allowing for very precise temperature control over a very large area of the furnace. This is important as it allows for a large number of samples to be included in the furnace exposed to a uniform temperature environment. Four-inch diameter quartz tubes were used within the furnaces for containment of gas and samples within each furnace. Water cooled flanges were used to cool both ends of each tube. A photo of the furnace setup is shown in Figure 4.

Figure 4. Two large tube furnace setups used for alloy corrosion experiments

All-ceramic (aluminum oxide - alumina) sample holders were fabricated by McDanel Advanced Ceramic Technologies (Beaver Falls, PA) for use in these experiments. The use of ceramic as the holder material is important as it eliminates gas species reactions with the holder material, and so the only reactions that can take place within this system are with the alloy samples themselves. Corrosion samples were suspended from an alumina rod, and separated from each other by alumina spacers. The holders were designed to hold a very large number of samples (144 total), and for these experiments 48 alloy samples were included in each test. A total of six samples of each alloy were included in each test, where 3 samples were pulled after 500 hours and the second 3 samples were pulled after 1000 hours. An image of the sample holder is shown in Figure 5, including the various corrosion samples.

For each experiment temperature was measured using thermocouples (k-type) in three separate locations across the sample holder. This is shown in Figure 6, where thermocouples are shown across the width of the sample holder as well as along its length. In this way, the temperature was precisely known for all samples from each test. The pressure for each experiment was maintained around 1 atm using a constant flow of CO_2 into the furnace tube along with a valve on the exit side of the tube which maintained the desired internal tube pressure. A CO_2 flow rate of approximately 150 cc/min was used for the full duration of each experiment. Prior to the start of each experiment the system was checked for leaks by pulling a vacuum on the system after everything was sealed up and checking for leaks using a helium leak detection system.

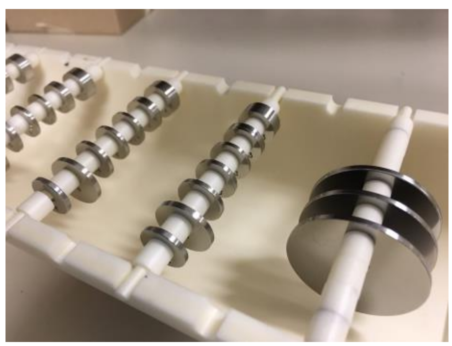

Figure 5. Aluminum oxide sample holder fabricated for the alloy corrosion experiments

Figure 6. Holder placement within the tube furnace along with thermocouple positions

3.3. Experimental Test Matrix

A total of six long duration corrosion experiments were planned as part of this work. A diagram for the full experiment test matrix is shown in Figure 7. Two experiments were completed in research grade CO_2, one at 350°C and the other at 600°C. Two experiment were also completed in industrial grade CO_2, at the same two temperatures. A final set of two experiments are being completed in air, at the same temperatures, to provide comparison for alloy behavior in terms of oxidation and carburization in an environment devoid of a carbon containing gas. In each of the six experiments the same set of eight alloys are included, and a consistent set of post-test analyses are completed for samples from each.

The use of both CO_2 gases in these experiments provide the means for evaluating alloy corrosion across the full spectrum of gas chemistry that will be possible for an SFR EC system. The use of the two test temperatures provides information about the effect of gas chemistry across the range of relevant system temperatures. This also provides insight into how alloy corrosion and carburization behavior changes across the range of system temperatures for these eight alloys.

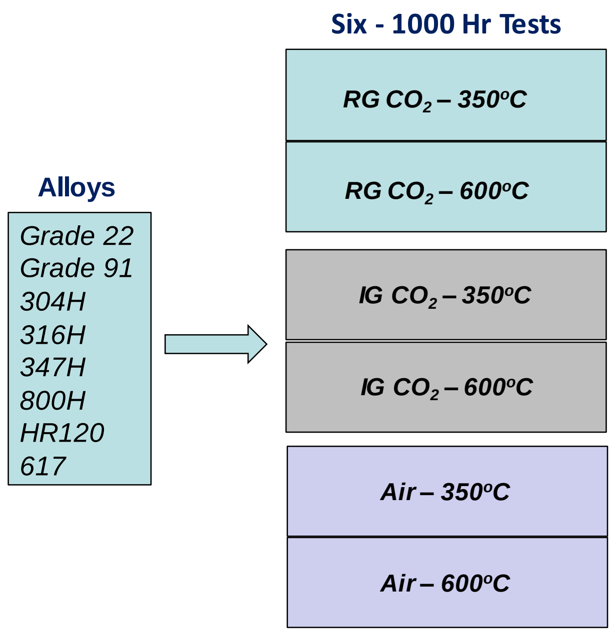

Figure 7. Matrix of corrosion experiments and alloys

3.4. Post-Test Sample Characterization

The approach to sample characterization was focused around understanding the influence of various factors (CO_2 gas chemistry and temperature) on the corrosion behavior and carburization behavior for a set of eight candidate alloys. As such, the main areas of characterization included here were sample weight change, metal loss, sample imaging / microscopy, and internal carburization. In this paper results are presented for a portion of these analyses (weight change and microscopy), and only for samples from the 4 experiments in CO_2 gases. Analyses for sample metal loss and internal carburization are described in this paper, but the results from these analyses are not yet complete. Also, while the two experiments in air have been completed, the analyses of samples from these are not provided in this report, as these are also still being completed.

3.4.1. Weight Change

Sample weight change, resulting from the 500 hour and 1000 hour CO_2 exposure durations, were measured using a Mettler-Toledo XP-26 Microbalance. Carefully measured initial sample dimensions were used to calculate the weight change per unit sample surface area, allowing the data to be normalized across the various sample geometries. The statistical analysis software JMP 12 was used to evaluate the influence of CO_2 gas chemistry and temperature on the weight change for the set of different alloys.

3.4.2. Metal Loss

After a detailed examination of literature describing alloy corrosion in supercritical CO_2 environments as part of the 2016 program [1] it appeared that all of the data was reported in terms of sample weight gain rather than in the more valuable format of metal loss. Metal loss refers to the reduction in unaffected (non-oxidized) alloy thickness that results from chemical corrosion reactions. It is significantly more valuable than weight gain data as it can be used to calculate corrosion rates (mm/year) and to make lifetime predictions.

Based on this, it seemed valuable to include an initial attempt at measuring alloy metal loss for samples subjected to CO_2 corrosion. Procedures are described for this in ASTM G1-03 "Standard Practice for Preparing, Cleaning, and Evaluating Corrosion Test Specimens" [9]. Here, a range of chemical cleaning solutions are recommended for Fe-base stainless steel alloys as well as for Ni-base alloys. Prior to using these cleaning solution to determine corrosion sample metal loss, they need to be evaluated for their effectiveness in removing the surface oxides. Here, it is important to determine the parameters (cycle time and number of cycles) at which the cleaning solutions will remove the surface oxide without removing the base metal itself.

Two solutions were selected for evaluation for each of these two alloy categories. For the Fe-base alloys, a nitric acid and a diammonium citrate cleaning solution are evaluated. For the lone Ni-base alloy (617), a hydrochloric acid and a sulfuric acid cleaning solution are evaluated. Following each prescribed cleaning cycle, samples are weighed to determine the weight loss from cleaning. For the Fe-base alloys a cleaning cycle is 10 minutes, while for the Ni-base alloys the cycle is 1 minute. For both types of alloys, a total of six cleaning cycles were used in this study.

To supplement this activity, separate coupons of many of the alloys were included into the second 500-hour portion of experiments in the test matrix. Specifically, 6 coupons for seven of the eight alloys (Grade 22, Grade 91, 316, 800H, 347, HR120, and 617) were exposed to RG CO_2 for 500 hours' duration at 350°C. A second set of 6 coupons for each of these alloys was exposed to RG CO_2 for 500 hours' duration at 600°C. The intention was to use these supplemental coupons to evaluate and optimize cleaning procedures that could later be used on the same coupons used for weight change measurements. An image showing the use of the supplemental coupons within the alumina sample holder is provided in Figure 8. Here, the supplemental coupons are rectangular, versus those for the weight change measurements which are round.

Figure 8. Sample holder showing the inclusion of supplemental metal loss coupons (rectangular)

3.4.3. Microscopy

Besides measuring the samples for weight gain and metal loss, it is important to also visually characterize the sample surfaces and oxidation layers. One sample of each alloy from each 1000-hour experiment is designated for microscopic evaluation. Prior to preparing samples for microscopy, images of each sample were taken using a KEYENCE Digital Microscope (VHX-6000).

Oxidation layers can be difficult to visually identify in cases where they are very thin. This is true for Ni-base alloys, and also for many alloys when exposed to lower temperatures (i.e. 350°C). In cases such as these, samples can be plated in copper to provide visual contrast between the oxidation layer and the sample mounting material (typically epoxy). This was done for all of the microscopy samples included in these experiments.

Prior to copper plating, sample surfaces were coated with a thin layer of gold. This was done to provide the electrically conductive surface necessary for copper plating. The gold sputtering was done with a PELCO SC-7 Auto Sputter Coater. Following gold coating, samples were electroplated with copper. The electroplating cell consisted of a copper working electrode (99.9% pure), an oxidized coupon counter electrode, and 150 mL of aqueous ~0.85 M copper sulfate pentahydrate solution. For the counter electrode, the thin layer of sputtered gold was contacted with an alligator clip so that plating of copper occurred preferentially on the outer surface. With working and counter electrodes immersed in solution, a BioLogic VSP-300 potentiostat was used to apply ~10 mA/cm^2 for 20-30 min to all samples, accounting for differences in surface area. From coulombic calculations, we estimate that the total amount of Cu plated from a two electron reduction process was 3.9 mg/cm^2. Non uniformities in the gold coating or oxidation layer, however, caused Cu plating to occur preferentially in areas that were better electrically connected.

After gold coating, the samples were prepared for analysis by mounting in epoxy, cross-sectioning, polishing. Samples were imaged with the LEICA DM 4000M microscope and LEICA DFC 500 camera at 50x and 100x magnification.

3.4.4. Internal Carburization

Besides measuring the internal carbon content for experiment test samples, hardness can be measured, providing an indication of internal carburization. Internal carbon content and hardness are well correlated due to carbon existing in the alloy as very hard metal carbides. So, an alloy with higher internal carbon concentrations will also have a higher measured hardness. Using the same samples from each alloy/experiment that were prepared for microscopic imaging, a hardness map can be constructed for each using nanoindentation techniques. Here, hardness is measured for a single 1000-hour sample of each alloy starting at the surface down to around 0.5 mm within the sample. In this way, it provides a comparison of internal carburization among the different alloys across the range of experimental conditions (gas chemistry and temperature).

4. RESULTS

Long duration experiments have been completed at 350°C and 600°C using both the RG and IG CO_2 gases. Three samples of each alloy have been extracted for analysis following 500 hours and 1000 hours' exposure, and weight change measurements are complete for these samples. Microscopic analysis has been completed for one sample of each alloy from the experiments in both IG and RG CO_2. Results from these samples are presented here.

Additional work is ongoing in several different areas, and information is also provided regarding the next steps in each of these. Samples from the four experiments in CO_2 are being characterized for metal loss as well as for internal carburization. Also, long duration experiments have been completed at 350°C and 600°C in air. Alloy samples from these experiments are being characterized for weight change, oxide microstructure, metal loss, and internal carburization.

4.1. Weight Change

Weight change data for the group of 8 alloys were examined with two overarching goals in mind. The first is to understand their corrosion behavior relative to each other in CO_2 at two temperatures relevant to an SFR EC system. The second is to determine if there is a statistically significant difference in the corrosion behavior of alloys for RG and IG $CO_{2,}$ also at these same two temperatures.

Regarding the relative corrosion behavior of the various alloys, data are shown in Figure 9 and Figure 10 for the two experiments at 350°C. Even at this low temperature, significantly greater weight gain was observed for the ferritic alloys than for the other six alloys. Out of these two ferritic alloys, F22 demonstrated significantly greater weight gain than F91. While the first chart includes the weight change for all 8 alloys, the second is included without the two ferritic alloys to better compare the other alloys amongst themselves. With IG CO_2 being the gas most likely to be used in a commercial system, it seems to make the most sense to compare alloys based on their behavior in this gas. Using this approach with the non-ferritic alloys in Figure 10, 316H demonstrated the greatest weight gain, while other alloys all demonstrated significantly lower weight gains. A final note here is that in both charts it appears that weight changes were modestly greater in IG CO_2 than for RG CO_2, although these changes are very minor.

Similarly, data are shown in Figure 11 and Figure 12 for the two experiments at 600°C. Not surprisingly, very large weight gains are now observed for the ferritic alloys. Considering the other alloys, 316H again demonstrated the highest weight gain, while the others demonstrated relatively similar gains. Differently than for the lower temperature, it now appears that weight changes were modestly greater in RG CO_2 than for IG CO_2, although these changes are again very minor. Referring back to Table 3, it is worth mentioning that the IG CO_2 cylinder used for the lower temperature experiment had higher impurity concentrations than for that used at the higher temperature test. It is unclear if this contributed to these results, and a detailed statistical analysis of these results was performed which provides a much clearer picture of this.

In order to determine if there is a statistically significant difference in the corrosion behavior of alloys for RG and IG $CO_{2,}$ at the two test temperatures, a detailed statistical analysis of the weight gain was completed. Sample population means for both gases were compared for each of the 8 alloys. This was done at both temperatures, using the 500-hour samples and also using the 1000-hour samples. Using the statistical software JMP12, an analysis of variance (Anova) was performed together with the Tukey-Kramer Honest Significant Difference (HSD) Test to identify if the difference between the population means were significant. An example for the output of this analysis is shown in Figure 13. In this chart, an example is provided (F22, 350°C, 1000-hours) for the case where the difference in weight gain for IG and RG gases is non-significant. In all instances the main outputs from the analysis are the Anova data (top) along with Mean Comparison data (bottom). The "Connecting Letters Report" at the very bottom provides the ultimate answer for whether a statistically significant difference exists between the two groups of data; populations not connected by the same letter are significantly different. A summary of this for all of the alloys is shown in Table 4. Significant difference was only observed for a small subset of the samples (4 of the 32 total scenarios), indicating that the gas chemistry has very little influence on the corrosion of these 8 alloys at the two temperatures.

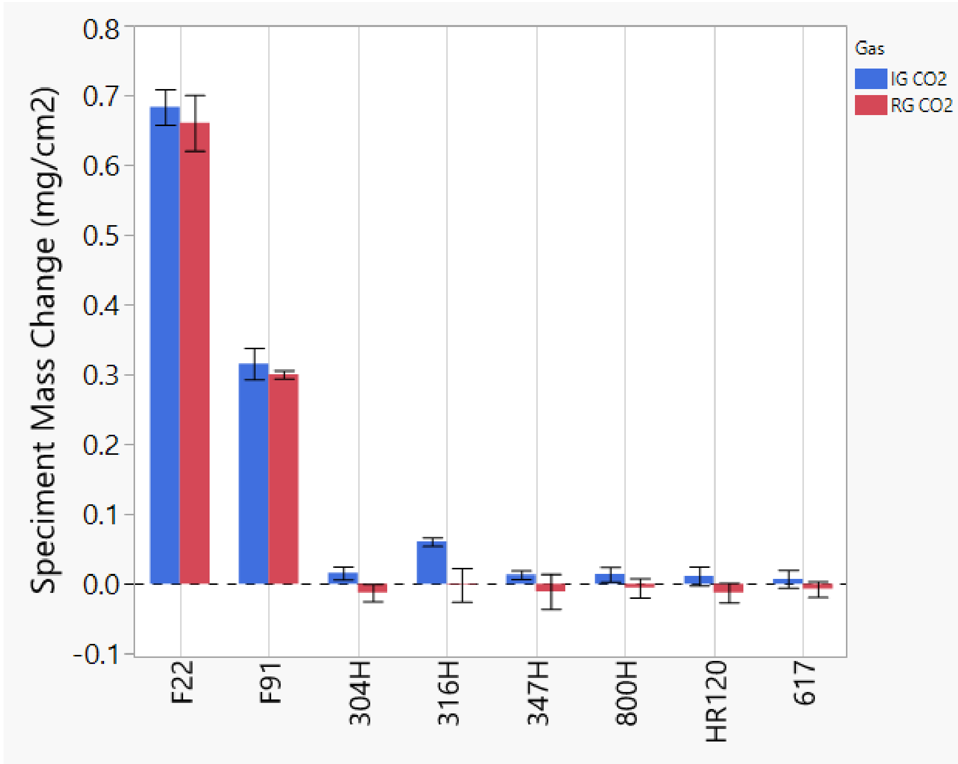

Figure 9. Specimen mass change for 8 alloys exposed at 350°C for 1000 h in different CO_2 gases

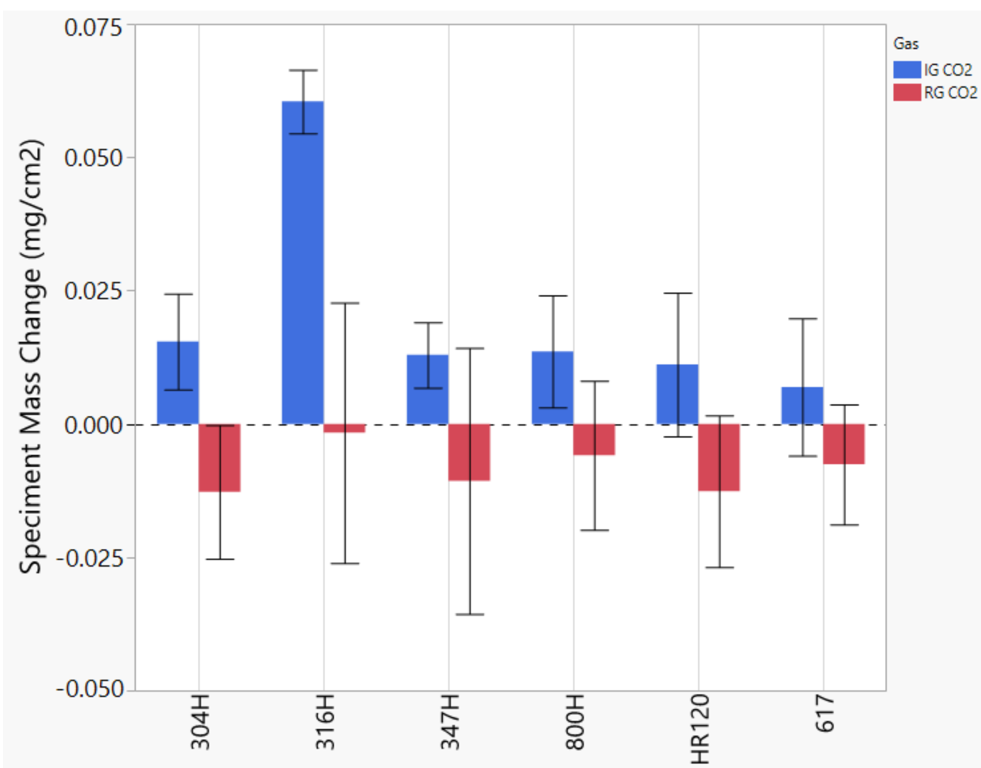

Figure 10. Specimen mass change for 6 alloys exposed at 350°C for 1000 h in different CO_2 gases

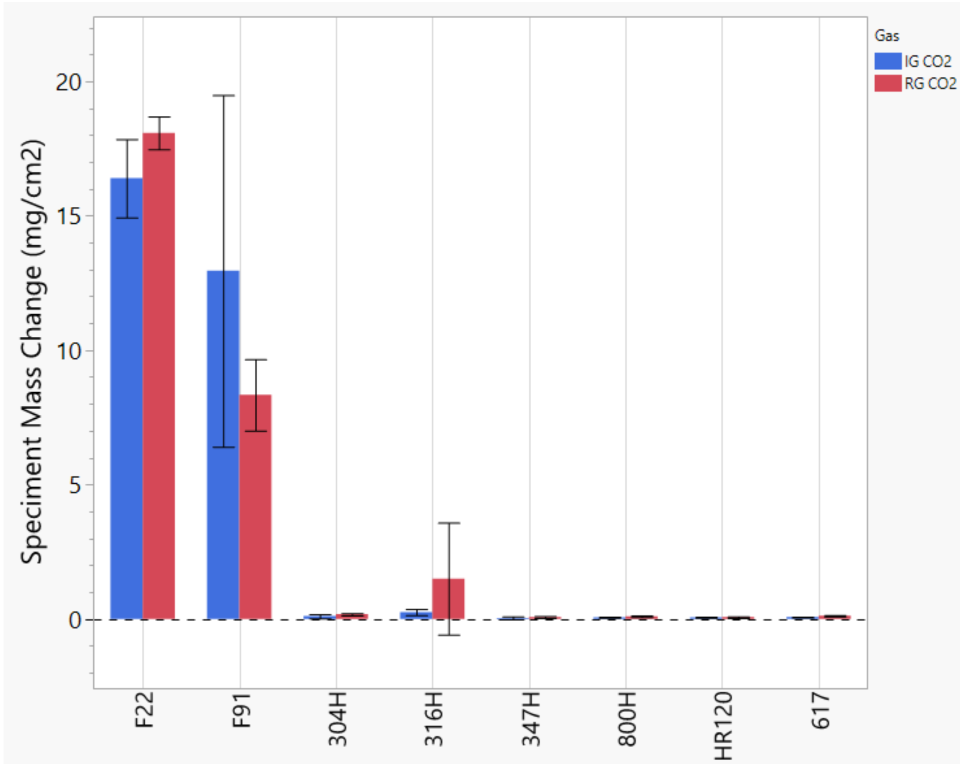

Figure 11. Specimen mass change for 8 alloys exposed at 600°C for 1000 h in different CO_2 gases

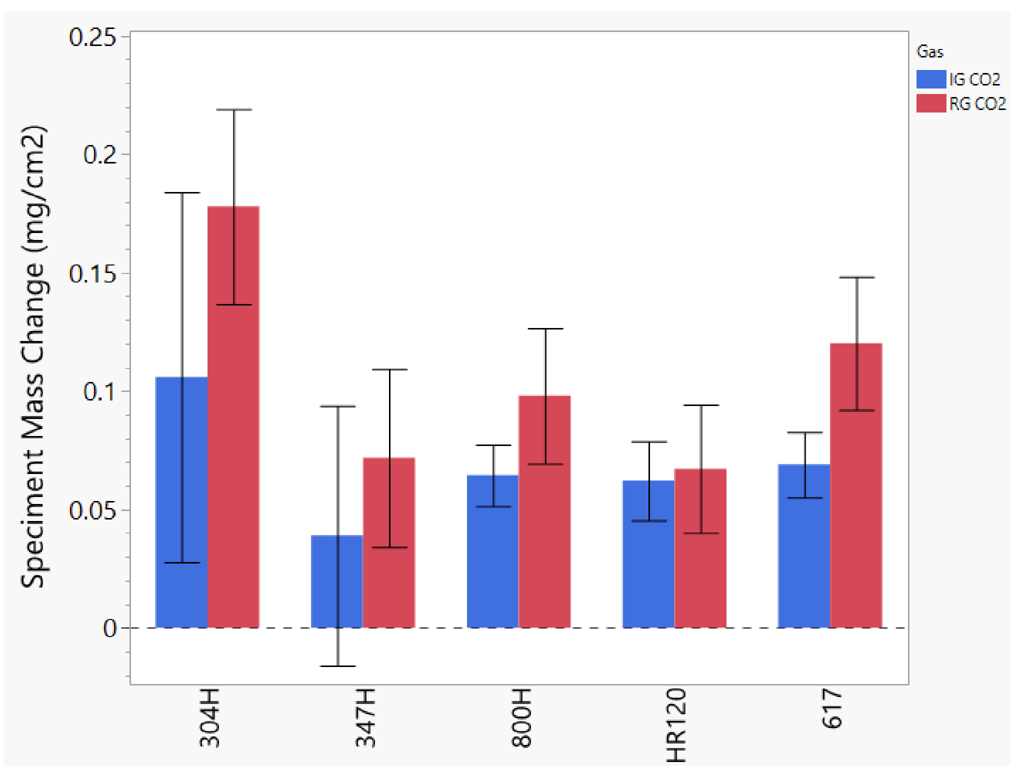

Figure 12. Specimen mass change for 5 alloys exposed at 600°C for 1000 h in different CO_2 gases

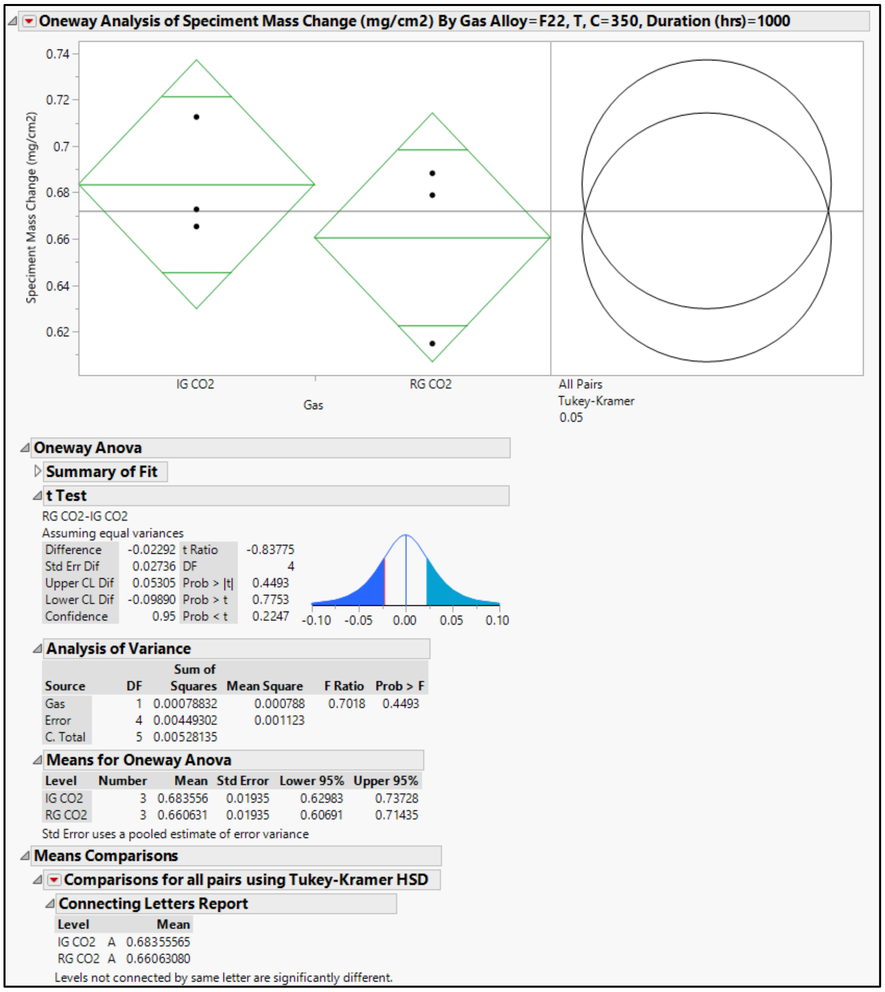

Figure 13. Statistical analysis data comparing weight gain data for F22 at 350°C in RG and IG CO_2

Table 4. Statistical Analysis Summary of Alloy Weight Change Differences for RG and IG CO_2

Alloy	350°C		600°C	
	500 hrs	1000 hrs	500 hrs	1000 hrs
F22	IG = RG	IG = RG	IG = RG	IG = RG
F91	IG = RG	IG = RG	IG = RG	IG = RG
304H	IG = RG	IG = RG	IG = RG	IG = RG
316H	IG > RG	IG > RG	IG = RG	IG = RG
347H	IG = RG	IG = RG	RG > IG	IG = RG
800H	IG = RG	IG = RG	IG = RG	IG = RG
HR120	IG = RG	IG = RG	IG = RG	IG = RG
617	IG = RG	IG = RG	IG = RG	RG > IG

4.2. Microscopy

Digital images of the surface of each alloy from the four CO_2 experiments are shown in Figure 14. Here, visual comparison is provided for each alloy at both temperatures in the two different CO_2 grades. Most notable from this are how different many of the 600°C alloys look between the two gases, while the differences are much less noticeable at 350°C.

Light microscope images of 1000-hour sample cross-sections were captured for samples of each alloy from the tests in IG and RG CO_2. Samples from the test at 350°C are shown in Figure 15, while those from the 600°C test are shown in Figure 16. The pinkish-orange layer at the top of each image is the copper that was plated on the surface of the samples. The lighter gray layer below this is the base metal, while the darker gray layer that for some samples is evident between the two is the oxidation layer.

At the lower temperature, a visible oxide layer was only observed for the alloys F22, F91, 304H and 347H. The oxide appeared to be similar thickness for both F22 and F91, and was significantly thicker than for the other alloys. A visible oxide layer was observed for each of the alloys at the higher temperature. In general, the oxide thicknesses appear to be a bit thicker now with the higher temperature. In the case of the F22 and F91 alloys, the oxide layer thickness is now dramatically thicker than for the lower temperature, increasing from around 10μm to around 100μm.

In comparing alloy oxidation characteristics for samples in IG CO_2 versus that in RG CO_2 at the two temperatures, there appears to be very little noticeable difference in oxide layer thicknesses among samples in the two gases. This supports the weight change observations and its associated statistical analyses that indicated non-significant differences between alloy corrosion in the two gases.

4.3. Next Steps

Additional work is ongoing in several different areas, and information is provided here regarding the next steps in each area. A final set of two 1000-hour experiments have recently been completed for the same alloys at the same two temperatures using air. Samples from these experiments are being characterized for weight change, metal loss, microscopy, and internal carburization.

For the experiments that have already been completed using CO_2, additional analyses are being conducted to determine internal carburization. Also, samples from all four of these experiments are being evaluated for metal loss in an attempt to make lifetime predictions for each alloy. Initial investigations are underway to evaluate a range of cleaning solutions using the supplemental samples that were included into the tests for these purposes.

Using the information from these additional analyses, together with the results presented in this paper, information will be provided to design engineers that enable appropriate alloy selections for system components. This is valuable in that it considers not only alloy weight gain in making alloy selections, but also the more valuable metal loss data in addition to the often overlooked internal carburization of alloys

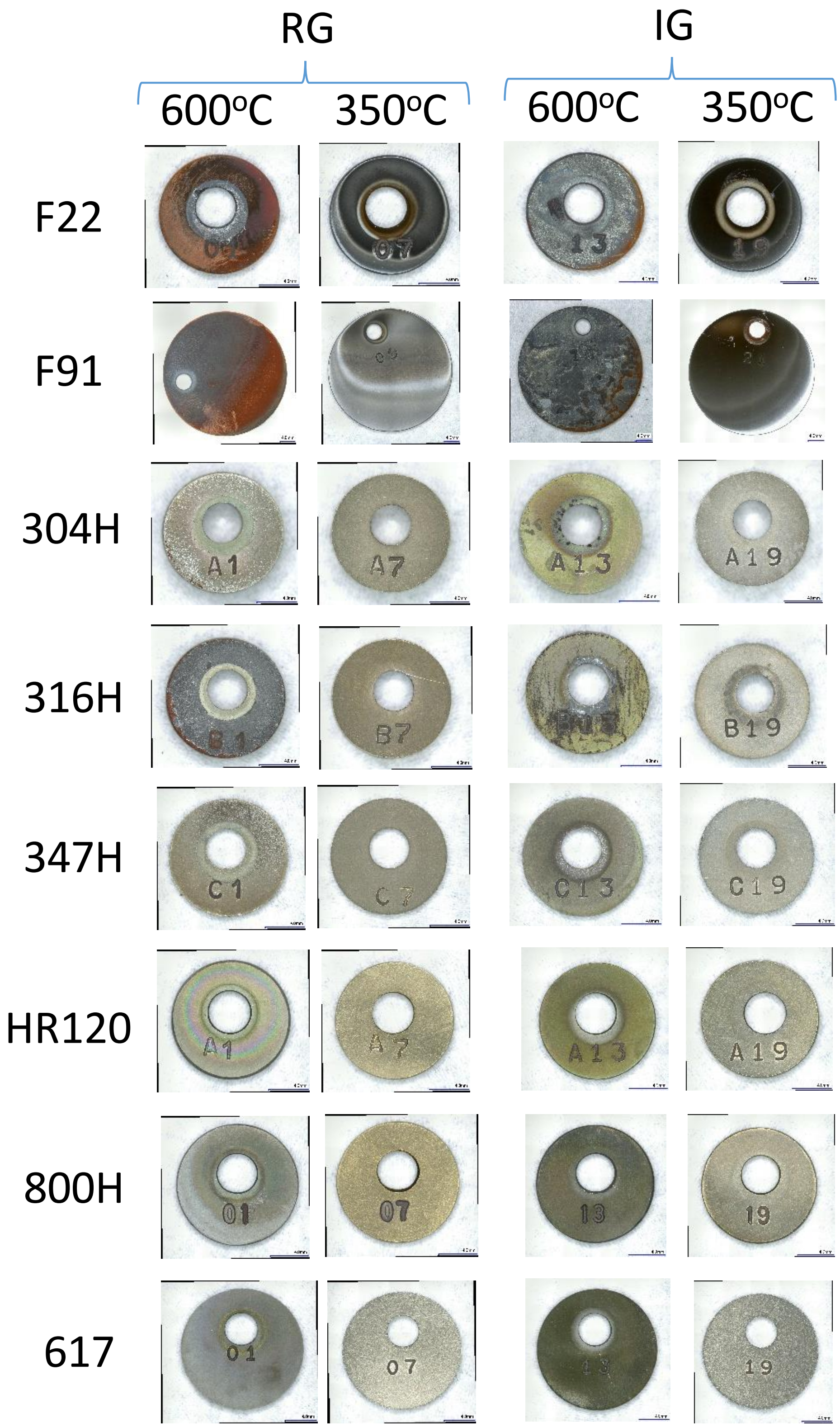

Figure 14. Digital microscope images of each alloy from the RG and IG CO_2 Experiments

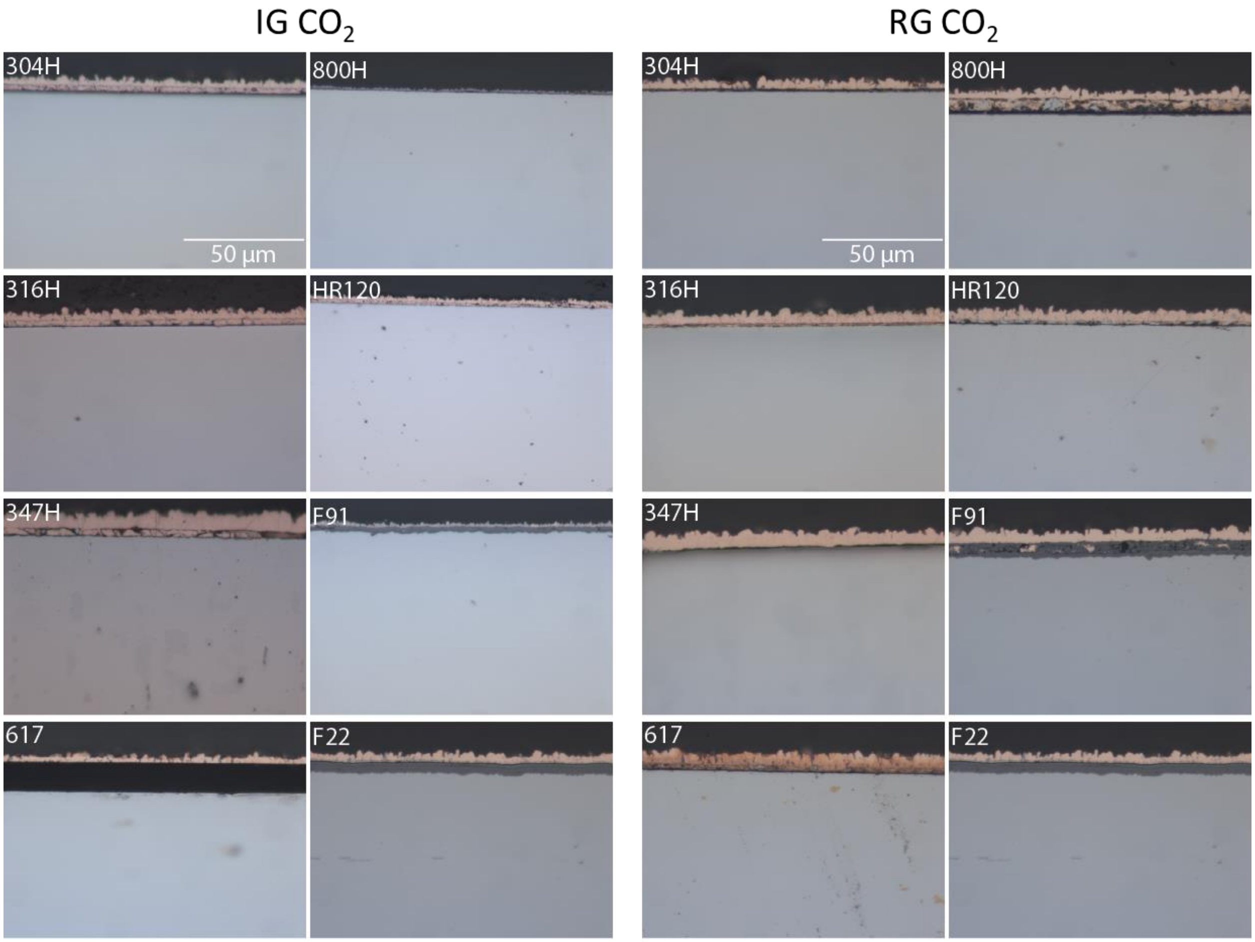

Figure 15. Polished cross-sections of each alloy in IG and RG CO_2 at 350ºC for 1000h

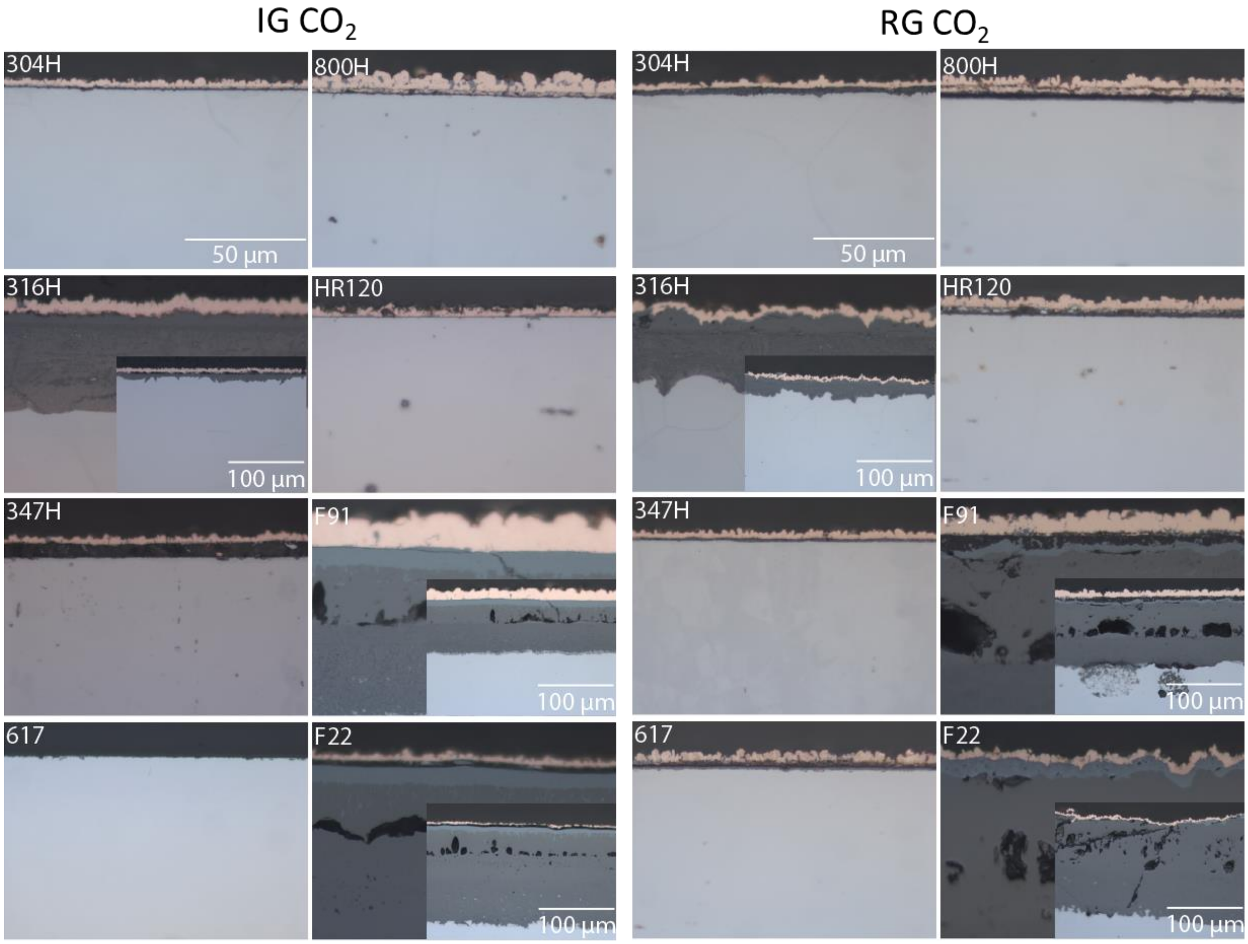

Figure 16. Polished cross-sections of each alloy in IG and RG CO_2 at 600ºC for 1000h

5. SUMMARY

An experimental program has been established that is systematically addressing four areas of risk associated with alloy recommendations for SFR EC system components. A summary of the results and/or status of each of these four areas of risk are summarized here:

(1) Alloy corrosion data has predominantly been obtained using research grade CO_2, while the lower purity industrial grade CO_2 will be used in a real system

Long duration (1000-hour) corrosion data has been obtained for 8 alloys at two temperatures relevant to an SFR EC system (350°C and 600°C) in both RG and IG CO_2. Statistical analysis was performed using this alloy weight change data in order to identify statistically significant differences in corrosion behavior for the two gases. Very little change in alloy corrosion behavior was observed for these two temperatures between RG and IG gases. Supporting this are microstructural analyses which indicate very little difference in oxide thicknesses for alloys in the two gases. It is yet unclear if gas chemistry has an influence on the other aspect of alloy corrosion, internal carburization. Investigations to understand this aspect of alloy corrosion are underway.

(2) There is very limited alloy corrosion data available at lower temperatures relevant for sodium fast reactor (SFR) energy conversion system applications

Long duration (1000-hour) corrosion data has been obtained for 8 alloys at two temperatures relevant to an SFR EC system (350°C and 600°C). Prior to this work, corrosion data was not available for this set of 8 candidate alloys at 350°C. This is particularly valuable for the two ferritic alloys as they were viewed as being candidates at these low temperatures (<400°C). Through this study, F22 and F91 were found to have significantly higher weight gain than any of the other alloys at 350°C. Careful analysis is needed to understand if the tradeoff of lower cost for these will outweigh their higher corrosion rates. Also, noteworthy is the observation of significantly greater corrosion of 316H than for 304H at both temperatures, in both CO_2 gases. With both alloys having similar cost, this data supports the use of 304H in place of 316H for SFR EC system components.

(3) Alloy corrosion investigations have only considered surface oxidation and not internal carburization

Samples of each of the 8 alloys from long duration tests in three gases (IG CO_2, RG CO_2, and Air) and two temperatures (350°C and 600°C) are being evaluated for internal carburization using nanoindentation hardness techniques. In comparing the results in CO_2 with those in air, carburization resulting from the carbon containing gas can be identified relative to that in an environment devoid of this carbon. The results from these analyses will be valuable for understanding this important aspect of alloy corrosion that has oftentimes been overlooked by researchers. Furthermore, these will provide understanding for the impact of gas chemistry and temperature on internal carburization for this set of SFR EC system candidate alloys. In absence of these analyses, alloy recommendations are made on the basis of weight change alone, which doesn't take this important area into consideration.

(4) Structural alloy corrosion has only been evaluated in terms of sample weight gain, rather than by the more useful metric of metal loss

Samples of each of the 8 alloys from long duration tests in three gases (IG CO_2, RG CO_2, and Air) and two temperatures (350°C and 600°C) are being evaluated for metal loss in an effort to obtain corrosion rates and lifetime predictions for these alloys/environments. Initial investigations are underway to evaluate a range of cleaning solutions using supplemental samples that were included into the tests for these purposes. After identifying the appropriate sample "descaling" solution/s, alloy samples from the 1000-hour corrosion experiments will be "descaled" and evaluated for metal loss. If successful, this will provide important information necessary for determining alloy lifetime predictions for sCO_2 system alloys.

NOMENCLATURE

S-CO_2 = Supercritical Carbon Dioxide
US DOE-NE = United States Department of Energy – Nuclear Energy Division
RCBC = Recompression Closed Brayton Cycle
SFR = Sodium Fast Reactor
EC = Energy Conversion
TIT = Turbine Inlet Temperature
ASME = American Society of Mechanical Engineers
RG = Research Grade Gas
IG = Industrial Grade Gas
ppm = Parts Per Million
Anova = Analysis of Variance
HSD = Honest Significant Difference

ACKNOWLEDGEMENTS

Sandia National Laboratories is a multimission laboratory managed and operated by National Technology & Engineering Solutions of Sandia, LLC, a wholly owned subsidiary of Honeywell International, Inc., for the U.S. Department of Energy's National Nuclear Security Administration under contract DE-NA0003525. Special acknowledgements to Ken Stewart for his contributions to this work through the installation and setup of the tube furnaces. Also, I would like to acknowledge Jeff Chames, Andy Gardea, Forrest Gittleson, Ryan Nishimoto, and Heidy Vega for their valuable contributions through microscopy sample preparation and analysis.

REFERENCES

1. Walker, M., et al., Progress in Overcoming Materials Challenges with S-CO2 RCBCs: Final Report, Sandia Report: SAND2016-9774, 2016
2. Walker, M., et al., Material Compatibility Issues for Advanced Nuclear Reactor Supercritical CO_2 Energy Conversion Systems. Whitepaper Proposal to DOE-NE, October 2016
3. Lee, H.J., et al., Corrosion and carburization behavior of chromia-forming heat resistant alloys in a high-temperature supercritical-carbon dioxide environment, Corrosion Science, Vol. 99, 2015.
4. Olivares, R., et al., Alloys SS316 and Hastelloy-C276 in Supercritical CO2 at High Temperature, Oxidation of Metals, Vol. 84, 2015.
5. Pint, B. A., The effect of O_2 and H_2O on Oxidation in CO_2 at 700^o – 800^{o}C, 5th International Symposium – Supercritical CO_2 Power Cycles, San Antonio, Texas, March 2016.
6. Holcomb, G.R., Dogan, O.N., Materials Performance in Supercritical CO_2 in Comparison with Atmospheric Pressure CO_2 and Supercritical Steam, 5th International Symposium – Supercritical CO_2 Power Cycles, San Antonio, Texas, March 2016.
7. Mahaffey, J., Anderson, M., Sridharan, K., Effect of Oxygen Impurity on Corrosion in Supercritical CO_2 Environments, 5th International Symposium – Supercritical CO_2 Power Cycles, San Antonio, Texas, March 2016.
8. Pint, B. A., The Effect of Temperature and Pressure on Supercritical CO2 Compatibility of Conventional Structural Alloys, 5th International Symposium – Supercritical CO_2 Power Cycles, San Antonio, Texas, March 2016.
9. American Society for Testing and Materials (ASTM). (2011). "Standard Practice for Preparing, Cleaning, and Evaluating Corrosion Test Specimens." *G1-03*, Philadelphia.